J Electroceram (2006) 16:425–430
DOI 10.1007/s10832-006-9892-2

Ferroelectric properties of heterolayered lead zirconate titanate thin films

Fransiska Cecilia Kartawidjaja · Zhaohui Zhou · John Wang

Abstract Heterolayered $Pb(Zr_{1-x}Ti_x)O_3$ thin films consisting of alternating $PbZr_{0.7}Ti_{0.3}O_3$ and $PbZr_{0.3}Ti_{0.7}O_3$ layers were successfully deposited via a multistep sol-gel route assisted by spin-coating. These heterolayered PZT films, when annealed at a temperature in the range of 600–700°C show (001)/(100) preferred orientation, demonstrate desired ferroelectric and dielectric properties. The most interesting ferroelectric and dielectric properties were obtained from the six-layered PZT thin film annealed at 650°C, which exhibits a remanent polarization of 47.7 $\mu C/cm^2$ and a dielectric permittivity of 1002 at 100 Hz. Reversible polarization constituents a considerably high contribution towards the ferroelectric hysteresis of the heterolayered PZT films, as shown by studies obtained from C-V and AC measurement.

Keywords Heterolayered PZT thin films · Sol-gel · Ferroelectric behaviors · Domain pinning

1 Introduction

Lead Zirconate Titanate ($Pb(Zr_{1-x}Ti_x)O_3$ or PZT) thin films, which exhibit excellent electrical properties including a high remanent polarization, high dielectric permittivity, and a large piezoelectric response, have received much attention for several technologically significant applications, such as for non-volatile memories, sensors, piezoelectric microactuators, and microelectromechanical systems [1, 2]. The most desirable ferroelectric properties are particularly found in PZT with composition near to the morphotropic phase boundary ($x \sim 0.45$–0.5), which separates the rhombohedral (Zr-rich PZT) and tetragonal (Ti-rich PZT) phases [1, 6]. Recently, extensive investigations have been made into heterolayered and multilayered PZT thin films, whereby several unique ferroelectric behaviors have been demonstrated [2–5]. Undoubtedly, the much improved electrical properties arise from the interactions between the alternating ferroelectric layers differing in either structure or composition or in both. The best known examples are the PZT films consisting of alternating rhombohedral and tetragonal layers, which have an overall composition close to the morphotropic phase boundary [3, 5].

PZT thin films have been successfully deposited by several processing techniques, including rf sputtering, ion beam deposition, metalorganic chemical vapor deposition (MOCVD), and sol-gel [1, 7]. Among them, sol-gel is of low cost, together with the flexibility of being able to control the film composition and film textures [8]. In this paper, we describe heterolayered PZT films consisting of alternating $Pb(Zr_{0.7}Ti_{0.3})O_3$and $Pb(Zr_{0.3}Ti_{0.7})O_3$ layers, synthesized via a multistep sol-gel route assisted by spin-coating. Their ferroelectric and dielectric properties are systematically investigated, in order to understand the processes that are responsible for the observed electrical behaviors, such as the reversible and irreversible polarizations in the heterolayered thin film structures.

2 Experiment procedures

The heterolayered PZT thin films were deposited via a multistep sol-gel route, assisted by spin coating. Two precursor solutions each with 10 mol% excess lead, namely $Pb(Zr_{0.7}Ti_{0.3})O_3$ (coded as $PZ_{70}T_{30}$) and $Pb(Zr_{0.3}Ti_{0.7})O_3$ (coded as $PZ_{30}T_{70}$), were prepared from $Pb(CH_3COO)_2$

F. C. Kartawidjaja · Z. H. Zhou · J. Wang (✉)
Department of Materials Science and Engineering, Faculty of Engineering, National University of Singapore, Singapore 117576
e-mail: msewangj@nus.edu.sg

$3H_2O$, $Zr[OCH(CH_3)_2]_4$, and $Ti[OCH(CH_3)_2]_4$. The starting materials were dissolved in a solvent mixture consisting of ethylene glycol monomethyl ether ($C_3H_8O_2$) and acetic acid (solvent volume ratio = 5/1.3). The concentration of the two sol solutions were controlled at 0.4 M. The $PZ_{70}T_{30}$ precursor solution was first spin-coated on the $Pt/Ti/SiO_2/Si$ substrate at 3000 rpm for 30 s to form the first layer, followed by drying at 300°C for 5 min by using hot plate, and baking at 500°C for 5 min by using RTP. The $PZ_{30}T_{70}$ precursor solution was then spin-coated as the second layer by following the same procedure. The procedure was repeated several times until up to six layers of alternating $PZ_{70}T_{30}$ and $PZ_{30}T_{70}$ were completed. The heterolayered PZT films were annealed at a temperature in the range of 600–700°C for 1 hour in a quartz furnace (Carbolyte) to realize the wanted perovskite structure. Phase identification and growth orientation of the heterolayered PZT films were characterized using XRD (D8 Advanced Diffractometer System, Bruker). Film textures and compositions were studied by using SEM and EDX (XL30 FEG Philips), while AFM was used to examine surface morphology. Their ferroelectric and dielectric properties were characterized using a ferroelectric analyzer (Radiant Technologies) and impedance analyzer (Solartron SI 1260, UK). For these electric measurements, a thin Au layer was dc sputter-deposited on the film top surface as the top electrode.

3 Results and discussion

Figure 1 shows the XRD traces of the six-layered PZT film consisting of alternating $PbZr_{0.7}Ti_{0.3}O_3$ and $PbZr_{0.3}Ti_{0.7}O_3$ layers, upon thermal annealing at 500°C and then at a temperature in the range of 600–700°C. The heterolayered PZT film annealed at 600, 650, and 700°C are coded as $PZ_{70}T_{30}$-600, $PZ_{70}T_{30}$-650, and $PZ_{70}T_{30}$-700 respectively. When $PZ_{70}T_{30}$ was chosen as the first layer for all these heterolayered thin films, they all show the wanted perovskite structure, where the rhombohedral structure of $PZ_{70}T_{30}$ and tetragonal structure of $PZ_{30}T_{70}$ are clearly shown. In addition, they all show a (001)/(100) preferred orientation. Indeed, both the stacking sequence of individual ferroelectric layers and thermal annealing schedule play important roles in determining the film orientation [2–4]. In particular, the first PZT layer can act as the nucleation site for the upper PZT layers [2, 4]. A minor amount of pyrochlore phase, as indicated by the diffraction peak at 2θ of 29.63° was observed for the heterolayered PZT film thermally annealed at 500°C in RTP. Upon annealing at 600°C, the pyrochlore phase had completely disappeared and the perovskite phase was the only phase detected by XRD.

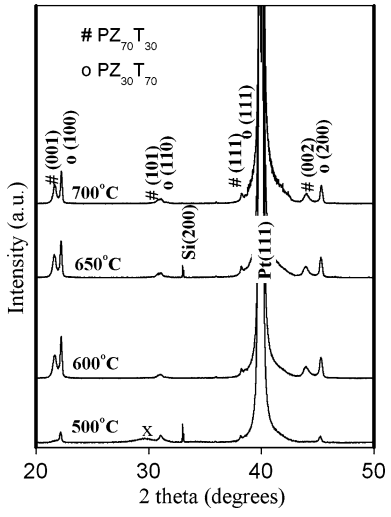

Fig. 1 XRD traces of the heterolayered PZT thin films upon annealing at 500°C and then at temperatures in the range of 600–700°C, with $PZ_{70}T_{30}$ as the first layer. x represents pyrochlore phase

Surface morphologies of the heterolayered films annealed at different temperatures are shown in Fig. 2. They exhibited a rosette structure, where an increase in annealing temperature promoted formation of such rosette structure. Indeed, such structure has been reported for PZT films derived from sol-gel, due to the lead deficiency arising from the loss at elevated temperatures [9–11]. The lead loss can occur as a consequence of the evaporation of Pb from the surface and/or the diffusion to the bottom electrode [9], giving rise to the rosette structure, where the film surface is inhomogeneous and rough. The process is dependent on Zr/Ti ratio in PZT thin films [12]. For example, the six-layered film consisting of $PZ_{70}T_{30}$ is rather different from that of $PZ_{30}T_{70}$, when both were annealed at 650°C. The $PZ_{70}T_{30}$ multilayer showed an extensive rosette structure, while $PZ_{30}T_{70}$ multilayer did not. This is consistent with the observation that less lead diffusion occurred in the titanium-rich PZT films [9]. The cross section of the six-heterolayered PZT film is shown in Fig. 3. There is no apparent inter-diffusion between the ferroelectric layer and the substrate. The film thickness is measured to be ~450 nm.

As shown in Figs. 4 and 5, the heterolayered PZT films demonstrate desired ferroelectric and dielectric properties. Figure 4 shows the effect of annealing temperature on the ferroelectric properties for the heterolayered PZT films. $PZ_{70}T_{30}$-650 shows the best ferroelectric and dielectric properties among the films studied in the present work, where a remanent polarization (P_r) of 47.7 $\mu C/cm^2$ and a coercive field (E_c) of 106 kV/cm were measured. The observed improvement in P_r value of $PZ_{70}T_{30}$-650 over that of $PZ_{70}T_{30}$-600 was attributed to the enhanced crystallinity as the annealing temperature increased. On the other hand, a rise in annealing temperature will increase the amount of lead loss as a result of surface evaporation, leading to formation of a rosette surface texture. This will affect the electrical properties of the PZT thin films. Thus, a drop in remanent

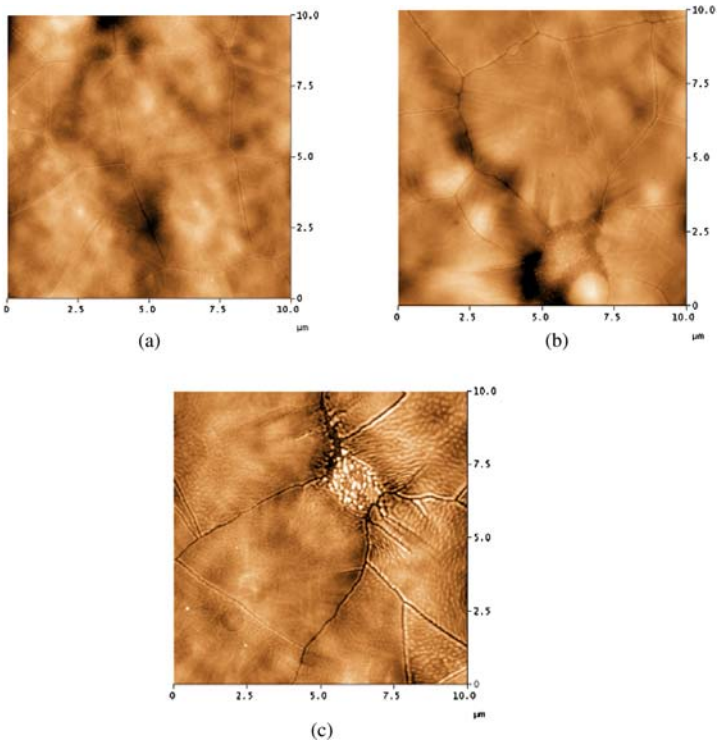

Fig. 2 Surface textures of the heterolayered thin films: (a) $PZ_{70}T_{30}$-600, (b) $PZ_{70}T_{30}$-650, and (c) $PZ_{70}T_{30}$-700 thin films

polarization P_r is observed for the heterolayered PZT film $PZ_{70}T_{30}$-700, which exhibited a P_r of 41.2 μC/cm^2 and a E_c of 125 kV/cm.

The heterolayered $PZ_{70}T_{30}$-650 thin film apparently shows a higher remanent polarization than that of the multilayered films (i.e., $PZ_{70}T_{30}$ multilayer and $PZ_{30}T_{70}$ multilayer) annealed at the same temperature, as shown in Fig. 4. $PZ_{70}T_{30}$ multilayer exhibits a P_r of 34.8 μC/cm^2 with a E_c value of 79.7 kV/cm, while $PZ_{30}T_{70}$ multilayer exhibits a P_r of 37.3 μC/cm^2 with a E_c value of 86.9 kV/cm. The enhancement in P_r for the heterolayered PZT thin film is due to the field induced stress and coupling effects between the layers of different structures [3, 5]. The $PZ_{70}T_{30}$ multilayer exhibits the lowest E_c value, suggesting that rhombohedral domains switch more easily as compared to those of tetragonal and orthorhombic domains. As shown in Fig. 5, heterolayered $PZ_{70}T_{30}$-650 demonstrates a significantly different dielectric permittivity as compared to those of the multilayered films. For example, $PZ_{70}T_{30}$ multilayer and $PZ_{30}T_{70}$ multilayer exhibit a respective permittivity of 560.9 and 539.3. The high dielectric permittivity observed for the $PZ_{70}T_{30}$ multilayer at low frequencies was related to the space charges, as confirmed by the high dielectric loss at low frequencies in connection with space charge relaxation and leakage.

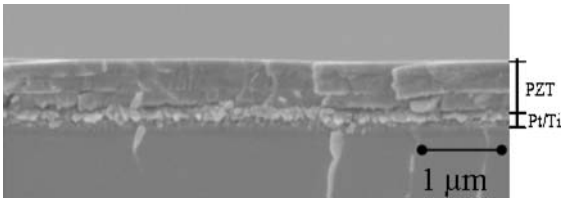

Fig. 3 Cross section of the six-heterolayered PZT thin film

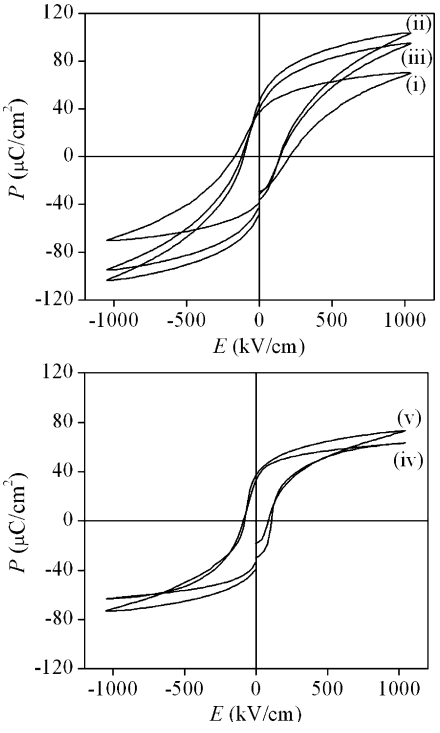

Fig. 4 Hysteresis loops of (i) heterolayered $PZ_{70}T_{30}$-600, (ii) heterolayered $PZ_{70}T_{30}$-650, (iii) heterolayered $PZ_{70}T_{30}$-700, (iv) $PZ_{70}T_{30}$ multilayer, and (v) $PZ_{30}T_{70}$ multilayer

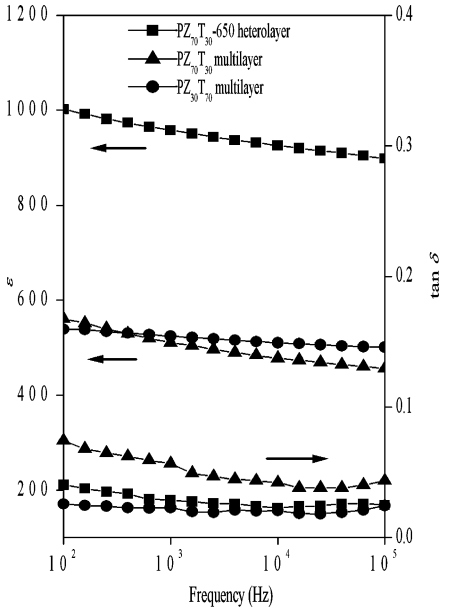

Fig. 5 Dielectric properties of the heterolayered and multilayered PZT thin films

Another interesting observation from the hysteresis loops of the heterolayered and multilayered PZT films is their differences in the reversible polarization. The combination of reversible and irreversible components in the presence of an external field constitutes the hysteresis of a ferroelectric material. There are several approaches to obtain information on the reversible and irreversible processes in a ferroelectric thin film. In the present study, two approaches were carried out, the first one of which is via C-V measurement. In this approach, the dielectric permittivity is measured by superimposing an ac electric field at a certain frequency over a range of dc electric field. The small applied ac signal will give rise to the reversible contribution of domain walls in the given dc field, since the external field is not big enough to drive the domain wall over a local maximum of the potential (the domain walls only move reversibly in the local maximum of the potential) [13, 14]. The C-V measurements of the three films are shown in Fig. 6, where the ε-E curves were measured at 1 kHz. Only one peak was observed for each curve when the dc field changes from the maximum negative value to the maximum positive value and vice versa. This peak corresponds to the reversal of 180° domains. The absence of a second peak, which is usually observed in PZT bulk ceramics, implies the limited switching of the non-180° domains in the PZT thin films [14, 15]. To study the contribution of reversible polarization towards the hysteresis for each film, the C-V curve was then integrated as polarization can be obtained by integrating the C-V curve, following the formula below

$$P_{\text{rev}} = \frac{1}{A}\int C(V)dV, \tag{1}$$

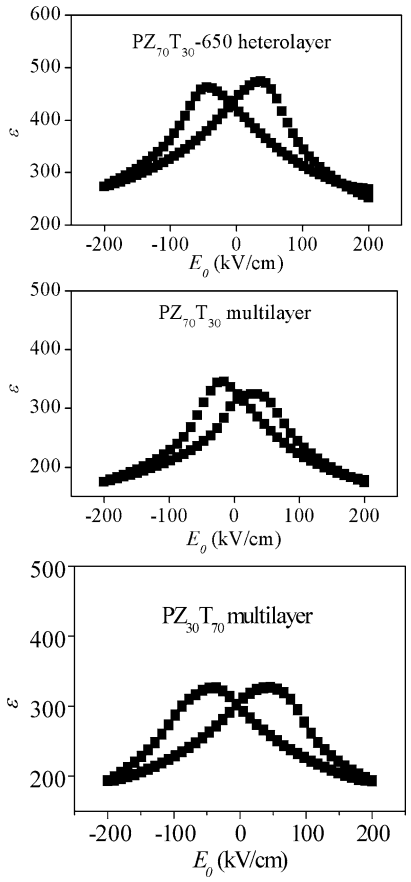

Fig. 6 Dielectric permittivity of the $PZ_{70}T_{30}$-650 heterolayer, $PZ_{70}T_{30}$ multilayer, and $PZ_{30}T_{70}$ multilayer as a function of field at a frequency of 1 kHz. The ac field is 0.5 V

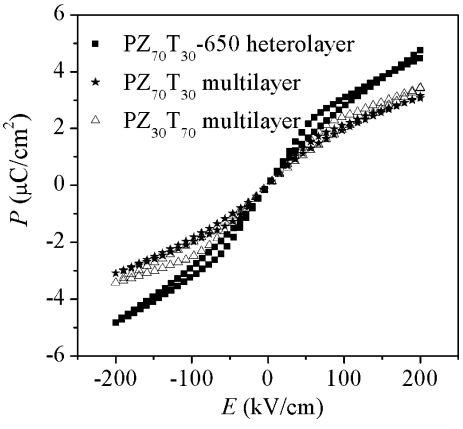

Fig. 7 Reversible polarization contribution in the $PZ_{70}T_{30}$-650 heterolayer, $PZ_{70}T_{30}$ multilayer, and $PZ_{30}T_{70}$ multilayer

where A is the area of sample and P_{rev} is the reversible polarization [13]. The resulting plots are shown in Fig. 7. Under the same measurement condition, heterolayered $PZ_{70}T_{30}$-650 apparently exhibits a higher reversible polarization as compared to the multilayered films. Among the multilayered thin films, $PZ_{30}T_{70}$ multilayer has a higher reversible polarization

than that of the $PZ_{70}T_{30}$ multilayer. The reversible polarization is related to the switching movement of 180° domains, while the irreversible polarization is mostly contributed by the reversal of non-180° domains which are ferroelectric and ferroelastic. These domains exhibit a higher mechanical strain due to the interaction with randomly distributed defects in the lattice, such as vacancies (domain pinning) [14, 16, 19]. This observation can be further confirmed by the second approach taken in this study, i.e., the Rayleigh law, which suggests that the domain wall contribution to the reversible and irreversible polarization can be described with the following formula:

$$\varepsilon = \varepsilon_{\text{init}} + \alpha E_0, \tag{2}$$

where $\varepsilon_{\text{init}}$ is the intrinsic lattice, reversible domain wall contribution, and αE_0 is the irreversible displacement of the walls [14, 16–18]. Figure 8 plots the dielectric permittivity of the three films as a function of applied ac field at different frequencies. They all show a linear relationship that follows the Rayleigh law. From these results, the value of $\varepsilon_{\text{init}}$ that corresponds to the reversible contribution and the

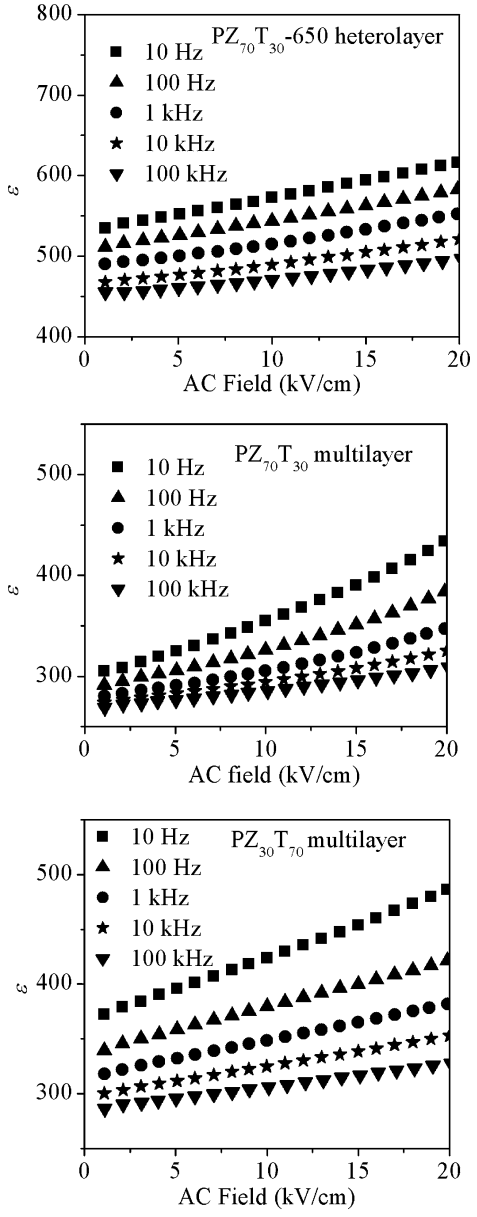

Fig. 8 Field dependences of dielectric permittivity for the $PZ_{70}T_{30}$-650 heterolayer, $PZ_{70}T_{30}$ multilayer, and $PZ_{30}T_{70}$ multilayer at different frequencies

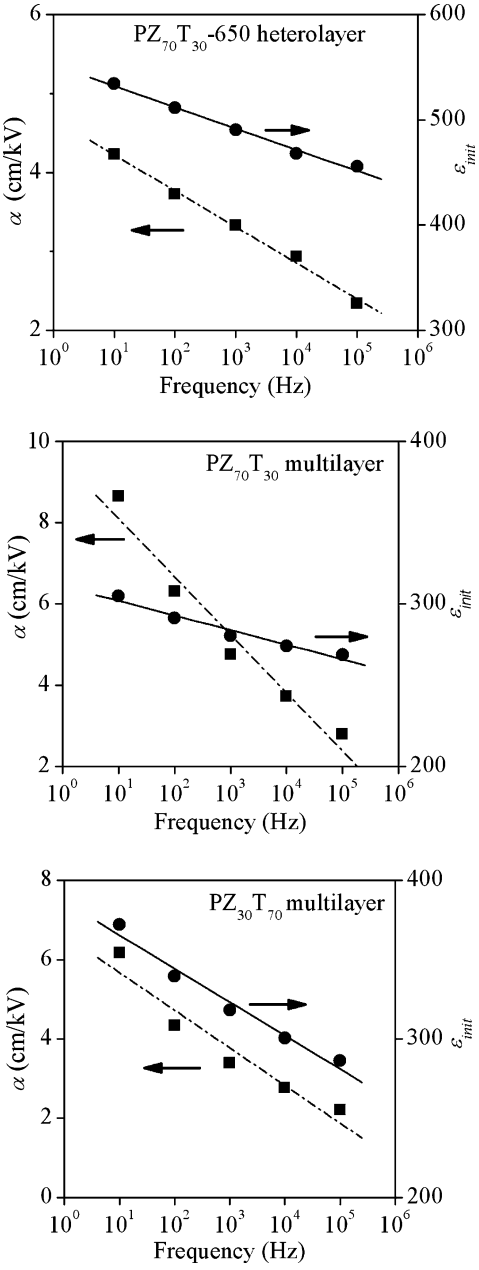

Fig. 9 Frequency dependences of the reversible and irreversible parameters ($\varepsilon_{\text{init}}$ and α) for the $PZ_{70}T_{30}$-650 heterolayer, $PZ_{70}T_{30}$ multilayer, and $PZ_{30}T_{70}$ multilayer, according to the Rayleigh law

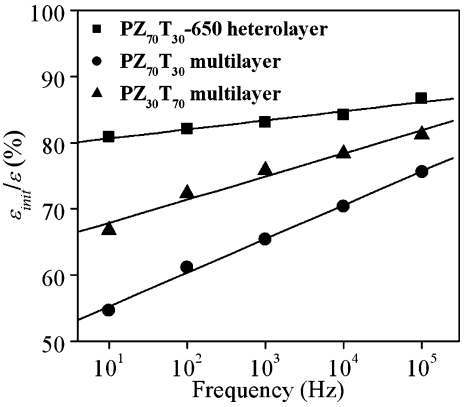

Fig. 10 Reversible domain wall contribution towards the dielectric permittivity as a function of the logarithm of frequency at an ac field of 20 kV/cm

value of α that corresponds to the irreversible contribution can be calculated. The resulting plots are shown in Fig. 9, where $\varepsilon_{\text{init}}$ and α are plotted against logarithm of frequency for each thin film. The contribution of reversible polarization towards the total dielectric permittivity is further shown in Fig. 10, where the ratio of $\varepsilon_{\text{init}}/\varepsilon$ is plotted against the logarithm of frequency. The $\varepsilon_{\text{init}}/\varepsilon$ ratio shows a similar trend as the results from the C-V measurement. The domain movement in the heterolayered film is less restricted, due to a bigger grain size as compared to those of the multilayered thin films. Thus, the heterolayered film has a higher $\varepsilon_{\text{init}}$. It is observed that $PZ_{70}T_{30}$-650 heterolayers exhibits the lowest α value ($\sim$4.58 cm/kV at 10 Hz), followed by the $PZ_{30}T_{70}$ multilayer and $PZ_{70}T_{30}$ multilayer. This observation suggests a domain wall pinning process in the $PZ_{70}T_{30}$-650 heterolayer, where the domains interact with defects and vacancies. As a result of the coupling between different ferroelectric layers in the heterolayered film, stresses can be generated at the interfaces during both sintering process and at application of an external electric field. In addition, it is likely that various defects are concentrated at the interfaces between different ferroelectric layers in the heterolayered thin films.

4 Conclusions

Heterolayered PZT thin films, consisting of alternating $PbZr_{0.7}Ti_{0.3}O_3$ and $PbZr_{0.3}Ti_{0.7}O_3$ layers, have been successfully synthesized via a multistep sol-gel route, assisted by spin coating. They showed a strong (001)/(100) preferred orientation and much improved ferroelectric and dielectric properties over the multilayered films. The most interesting ferroelectric and dielectric properties were obtained from the six-heterolayered PZT thin film annealed at 650°C, which shows a remanent polarization of 47.7 μC/cm^2 and a dielectric permittivity of 1002 at 100 Hz. The much improved ferroelectric and dielectric properties are attributed to the filed-induced coupling between the different layers in heterolayered films. The heterolayered PZT and multilayered PZT films show a significant difference in the reversible polarization. Under a sub-switching field, the reversible polarization in the heterolayered film is higher than that of the multilayered films. A large contribution from the irreversible polarization ($\alpha \sim 4.58$ cm/kV at 10 Hz) is observed with the $PZ_{70}T_{30}$ heterolayer annealed at 650°C, due to domain pinning as a result of the interaction with defects and vacancies.

References

1. D. Shi, *Functional Thin Films and Functional Materials* (Springer, New York, 2001).
2. S.G. Lee, I.G. Park, S.G. Bae, and Y.H. Lee, *Jpn. J. Appl. Phys.*, **36**, 6880 (1997).
3. Z.H. Zhou, J.M. Xue, W.Z. Li, and J. Wang, *J. Appl. Phys.*, **96**, 5706 (2004).
4. K.T. Kim, C. Kim, and S.G. Lee, *Microeelectr. Eng.*, **66**, 662 (2003).
5. F.M. Pontes, E. Longo, and E.R. Leite, *Appl. Phys. Lett.*, **84**, 5470 (2004).
6. B. Jaffe, W.R. Cook, and H. Jaffe, *Piezoelectric Ceramics* (Academic Press Inc. (London) Ltd., New York, 1971).
7. G. Yi, Z. Wu, and M. Sayer, *J. Appl. Phys.*, **64**, 2717 (1988).
8. C.J. Brinker and G.W. Scherer, *Sol-Gel Science* (Academic Press Inc., London, 1990).
9. T. Atsuki, N. Soyama, G. Sasaki, T. Yonezawa, K. Ogi, K. Sameshima, K. Hoshiba, Y. Nakao, and A. Kamisawa, *Jpn. J. Appl. Phys.*, **33**, 5196 (1994).
10. G.A.C.M. Spierings, M.J.E. Ulenaers, G.L.M. Kampschoer, H.A.M. van Hal, and P.K. Larsen, *J. Appl. Phys.*, **70**, 2290 (1991).
11. V. Chikarmane, J. Kim, C. Sudhama, J. Lee, and A. Tasch, *J. Electron. Mater.*, **21**, 503 (1992).
12. J.W. Zhan, Y. Aoki, J.Y. Li, H. Kokawa, and R. Maeda, *J. Crystal Growth* **267**, 92 (2004).
13. D. Bolten, U. Bottger, and R. Waser, *J. Appl. Phys.*, **93**, 1735 (2003).
14. D. Damjanovic, *Rep. Prog. Phys.*, **61**, 1267 (1998).
15. N. Bar-Chaim, M. Brunstein, J. Grunberg, and A. Seidman, *J. Appl. Phys.*, **45**, 2398 (1974).
16. D. Damjanovic, *J. Appl. Phys.*, **82**, 1788 (1997).
17. D.V. Taylor and D. Damjanovic, *J. Appl. Phys.*, **82**, 1974 (1997).
18. D.V. Taylor and D. Damjanovic, *Appl. Phys. Lett.*, **73**, 2045 (1998).